OMTM, Volume *30*

Supplemental information

Development of new adeno-associated virus capsid variants for targeted gene delivery to human cardiomyocytes

Cindy Y. Kok, Shinya Tsurusaki, Marti Cabanes-Creus, Sindhu Igoor, Renuka Rao, Rhys Skelton, Sophia H.Y. Liao, Samantha L. Ginn, Maddison Knight, Suzanne Scott, Mario Mietzsch, Rebecca Fitzsimmons, Jessica Miller, Tamer M.A. Mohamed, Robert McKenna, James J.H. Chong, Adam P. Hill, James E. Hudson, Ian E. Alexander, Leszek Lisowski, and Eddy Kizana

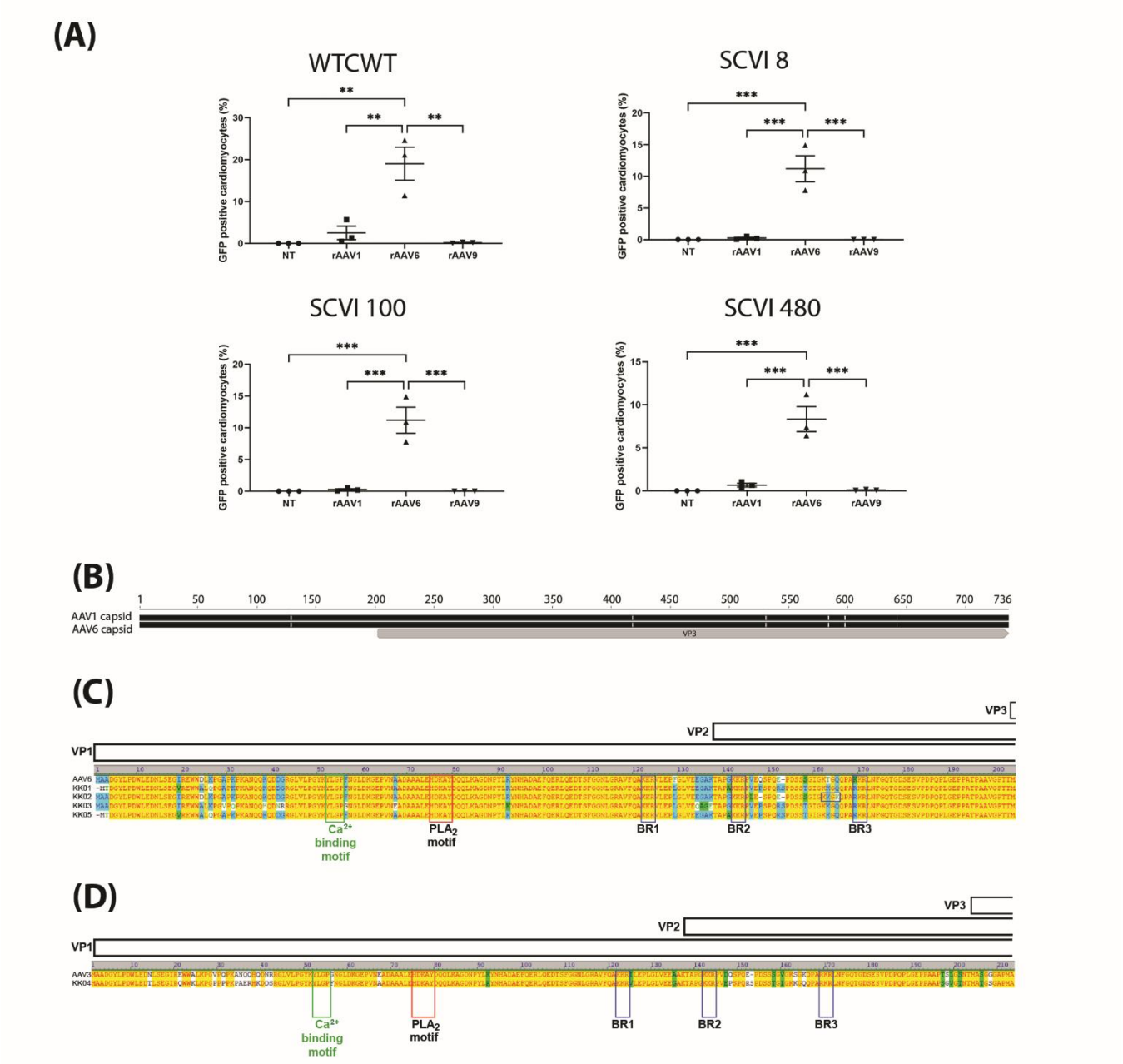

Figure S1: Comparison of transduction efficiency of cardiotropic rAAV capsids in hiPSC-CMs.

A) Four lines of hiPSC-CMs (WTCWT, SCVI 8, SCVI 100, SCVI 480) were transduced with rAAV.CBA.GFP vectors at MOT 1000, followed by analysis using flow cytometry to quantify GFP (n = 3 per group) on day 5 post transduction. Flow cytometry dot plots quantifying the proportions of GFP positive cardiomyocytes (cTnT+ cells). (B) Alignment of AAV1 and AAV6 capsids, showing amino acid differences within the VP3 region. (C) All novel variants except rAAV.KK04 were aligned to parental AAV6. (D) The amino acid sequence of rAAV.KK04 was aligned to parental AAV3. Statistical significance of differences was calculated using an ordinary one-way ANOVA, and the difference between the mean of the variants and AAV9 (for heart) or AAV8 (for liver) was calculated with Dunnett's multiple comparison test (** $p \leq 0.01$, *** $p \leq 0.001$).

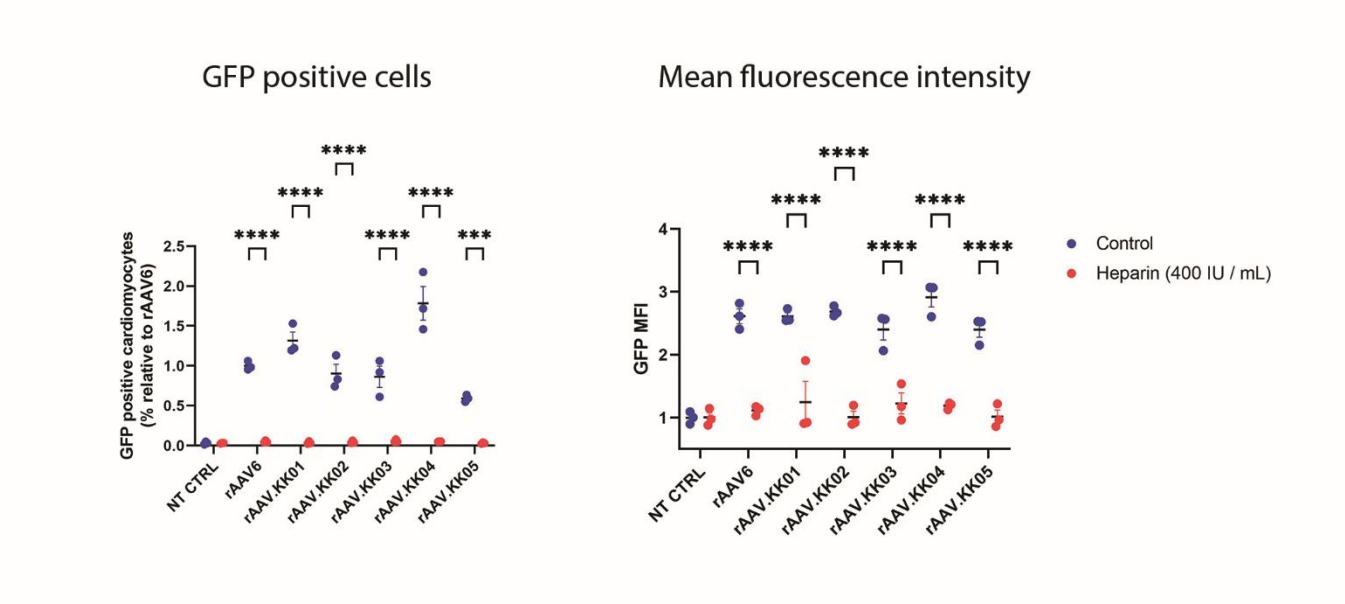

Figure S2: Novel AAV variants bind to soluble heparin, leading to reduced transduction efficiency in hiPSC-CMs

In vitro heparin competition assay using hiPSC-CMs (SCVI 8) transduced with rAAV6.CBA.GFP and rAAV.KK01-05.CBA.GFP at MOT 1000, with and without soluble heparin (400 IU / mL). Cells were then analysed by flow cytometry to quantify GFP on day 5 post transduction (SCVI 8, n = 3 per group). Results expressed as a fold reduction change to non-heparin rAAV6 (for GFP positive cells) or fluorescence of non-heparin NT (for mean fluorescence intensity). Statistical significance of differences was calculated using an ordinary two-way ANOVA, and the difference between the mean of control and heparin treated cells for each variant was calculated with Sidak's multiple comparison test (*** $p \leq 0.001$, **** $p \leq 0.0001$).

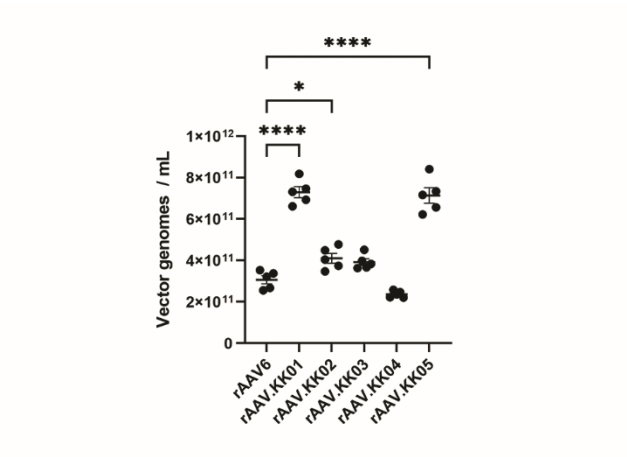

Figure S3: Manufacturability of novel capsids relative to AAV6. Comparison of titres from virus preps of rAAV.KK01-05 and rAAV6 packaged with a CBA-GFP cassette (rAAV.CBA.GFP). Five 15 cm dishes of HEK293T cells were used to package the viruses for each variant. Statistical significance of differences was calculated using an ordinary one-way ANOVA, and the difference between the mean of the variants and AAV6 was calculated with Dunnett's multiple comparison test (* $p \leq 0.05$, **** $p \leq 0.0001$).

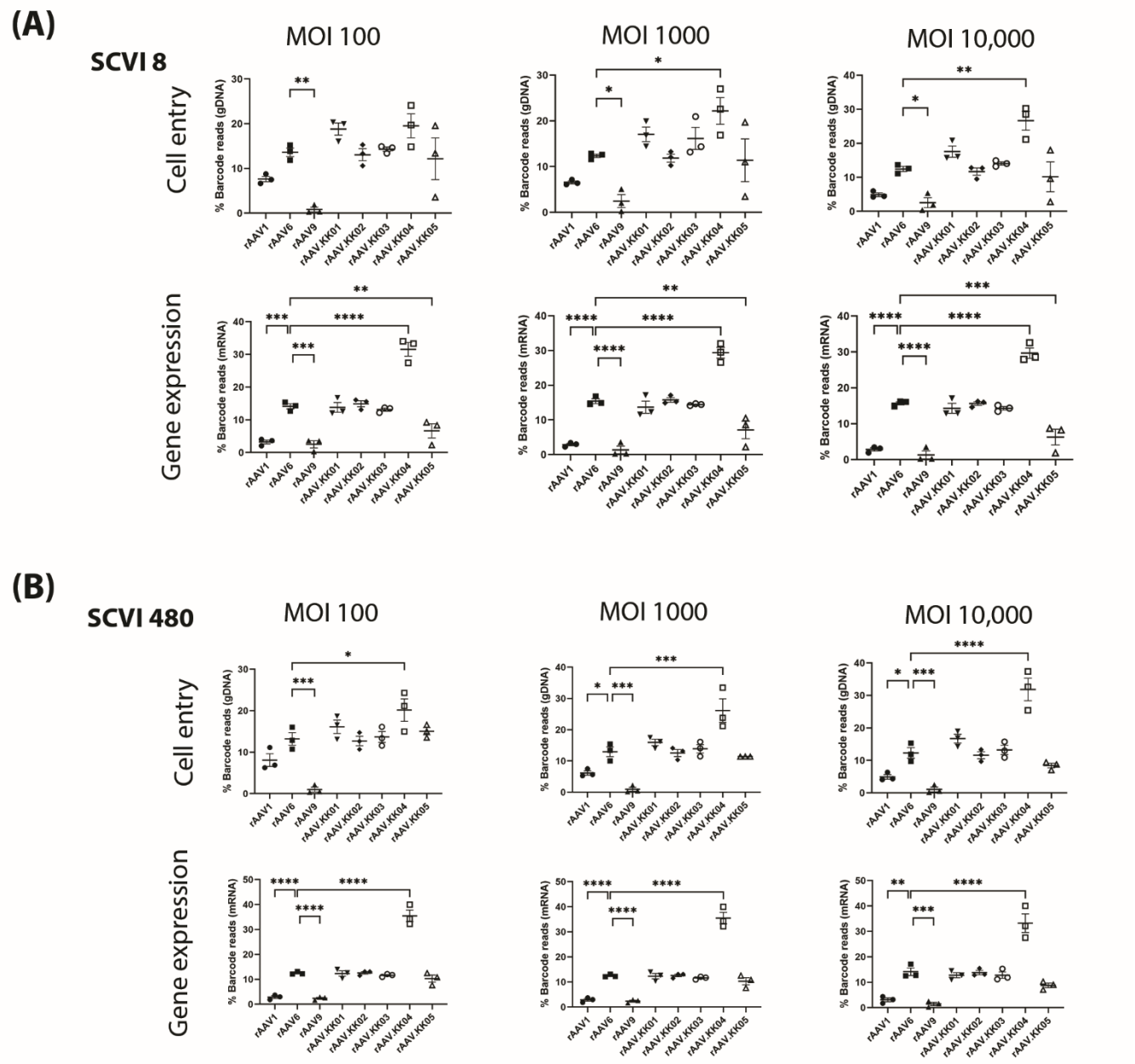

Figure S4: rAAV.KK04 was most efficient at gene delivery to hiPSC-CMs.

Two lines of hiPSC-CMs were competitively transduced with a barcoded library of rAAV.CMV.GFP vectors at MOT 100, 1000 and 10,000, then harvested at D5 post-transduction. Extraction of DNA/RNA was performed, followed by analysis using next generation sequencing (n = 3). The relative proportions of barcode reads post NGS analysis were given at the level of cell entry (gDNA) and gene expression (mRNA) for (A) SCVI 8 and (B) SCVI 480. Results were expressed as percentage of total reads for each cell line. See also Supplementary Figure 3. Statistical significance of differences was calculated using an ordinary one-way ANOVA, and the difference between the mean of the variants and AAV6 was calculated with Dunnett's multiple comparison test (* $p \leq 0.05$, ** $p \leq 0.01$, *** $p \leq 0.001$, **** $p \leq 0.0001$).

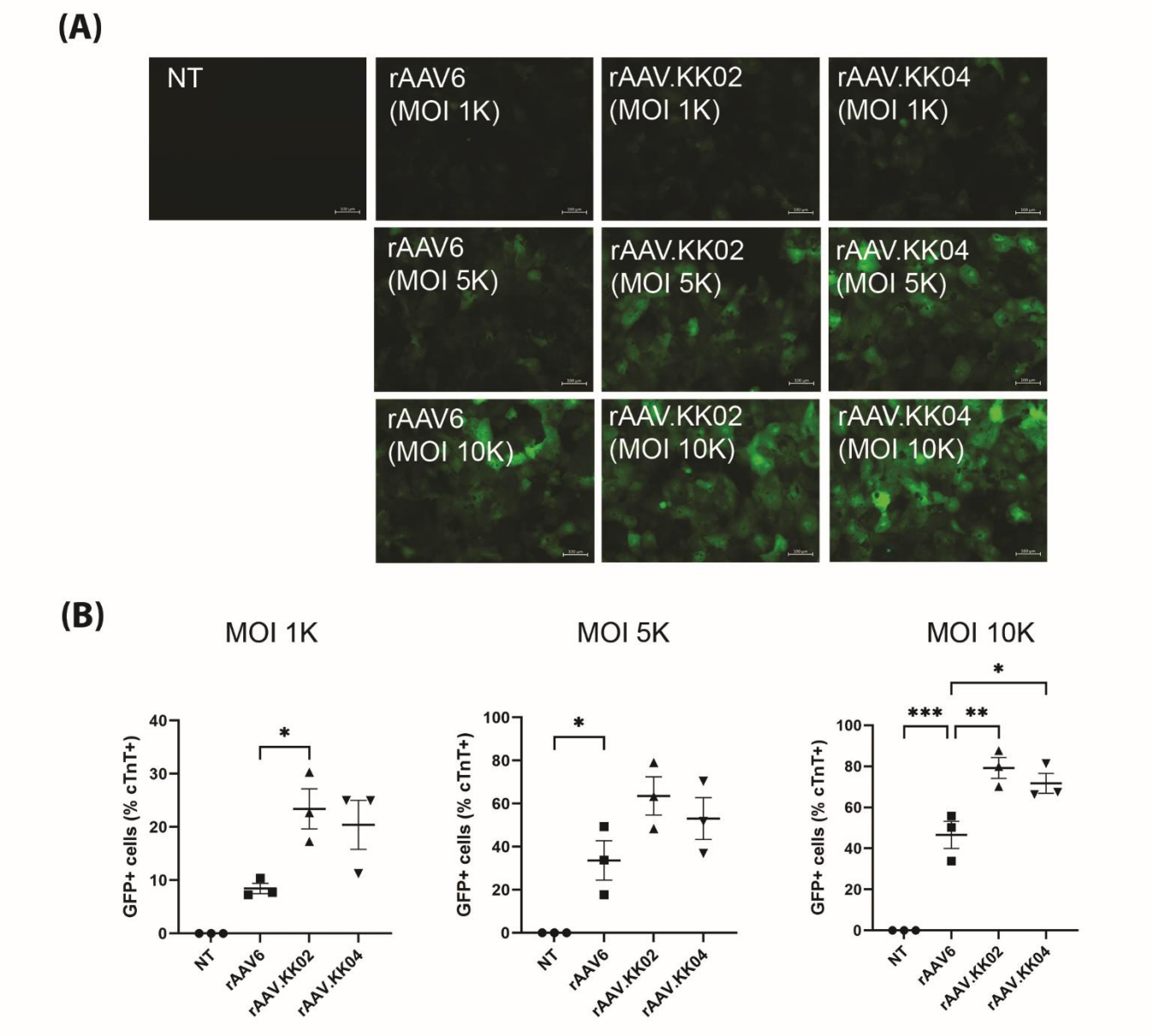

Figure S5: Changing the promoter from CBA to cTnT resulted in higher transduction efficiency of rAAV.KK02 and rAAV.KK04 relative to rAAV6. (A) hiPSC-CMs were transduced with unbarcoded rAAV.cTnT.GFP vectors at MOT 1000, followed by analysis using microscopy and flow cytometry to quantify GFP (n = 3 per group for SCVI 8) on day 5 post transduction. Fluorescence images showing GFP auto-fluorescence in live cells (scale bar = 100 uM). (B) Flow cytometry dot plots quantifying proportions of GFP positive cardiomyocytes (cTnT+ cells) in hiPSC-CMs. Statistical significance of differences was calculated using an ordinary one-way ANOVA, and the difference between the mean of the variants and AAV6 was calculated with Dunnett's multiple comparison test (* $p \leq 0.05$, ** $p \leq 0.01$, *** $p \leq 0.001$).

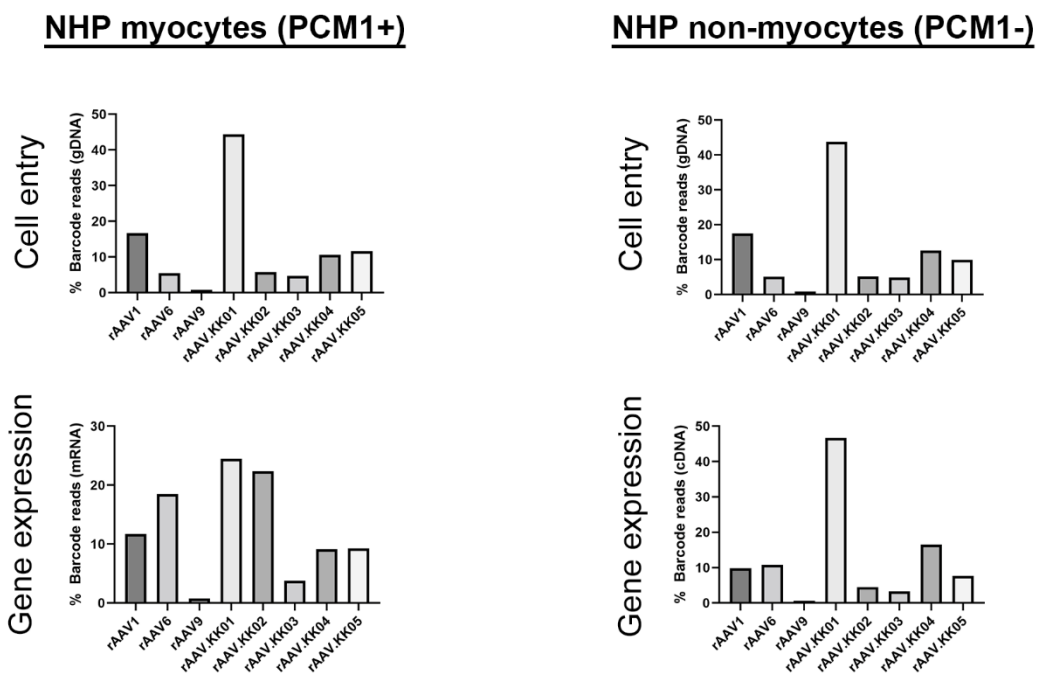

Figure S6: Comparison of rAAV transduction in non-human primate cardiac slices. Cardiac slices were generated from the left ventricular myocardium of a non-human primate. Slices were transduced with a barcoded library of rAAV.CMV.GFP vectors at MOT 10,000 (n = 1). Two days post transduction, DNA and RNA were extracted from the slices and analysed by next generation sequencing. The relative proportions of barcode reads post NGS analysis were given for whole heart and nuclear DNA/RNA at the level of cell entry and gene expression. Results were expressed as percentage of total reads for each condition.

Table S1: Script for ggplot used to generate Figure 7. See also Table S2 for data.

```
# install required packages that aren't already present
list.of.packages <- c("tidyverse", "readxl", "here")
new.packages <- list.of.packages[!(list.of.packages %in% installed.packages()[,"Package"])]
if(length(new.packages)) install.packages(new.packages)
```

```
# load libraries
library(tidyverse)
```

```
# read data from excel sheet
dna <- readxl::read_excel(("Fig7_data.xlsx"), range="B1:D69") %>%
  mutate(lib = "Expression - RNA")
rna <-  readxl::read_excel(("Fig7_data.xlsx"), range="G1:I69") %>%
  mutate(lib="Cell entry - DNA")
```

```
# order for axes
order_models <- rev(c("hiPSC-CM", "hCO", "Human CM 1", "Human CM 2", "NHP CM", "Pig CM",
"Mouse heart"))
order_aav <- c("rAAV1", "rAAV6", "rAAV8", "rAAV9", "rAAV.rh10", "rAAV.rh74", "rAAV.KK01",
"rAAV.KK02", "rAAV.KK03", "rAAV.KK04", "rAAV.KK05")
data <- bind_rows(dna, rna) %>%
  # change iPSC-CM to hiPSC-CM in RNA
  mutate(Model = case_when(
    Model == "iPSC-CM" ~ "hiPSC-CM",
    TRUE ~ Model
  )) %>%
  # change to factor for order on plot
  mutate(Model = factor(Model, levels=order_models)) %>%
  mutate(AAV = factor(AAV, levels=order_aav))
```

```
missing <- tibble(
  Model = rep(c("hiPSC-CM", "hCO","NHP CM"), 3),
  AAV = rep(c("rAAV8", "rAAV.rh10", "rAAV.rh74"), each=3)
) %>%
  mutate(text = "NA")
```

```
# make plot
data %>%
  ggplot(aes(x=AAV, y=Model)) +
  geom_point(aes(size=Ratio, color=Ratio)) +
  geom_text(data = missing, aes(label=text), size=3, color="black") +
  facet_grid(rows=vars(lib), scales="free") +
  scale_colour_gradient(
    low = "#dbf3ff",
    high = "#001345",
  ) +
  theme_bw(base_size=14) +
  theme(axis.text.x=element_text(angle=90, vjust=0.5, hjust=1)) +
  theme(axis.line = element_line(color='black'),
        plot.background = element_blank(),
        panel.grid.major = element_blank(),
```

```
        panel.grid.minor = element_blank(),)
# save plot
ggsave("Figure_7.pdf", height = 6, width=6)
```

Table S2: Summary data for rAAV variant performance at cell entry (DNA) and gene expression (RNA) across various screening platforms. Data used with R script (see also Table S1) for generating Figure 7

DNA			RNA		
AAV	Model	Ratio	AAV	Model	Ratio
rAAV1	iPSC-CM	6.55	rAAV1	hiPSC-CM	2.89
rAAV6	iPSC-CM	12.36	rAAV6	hiPSC-CM	15.42
rAAV9	iPSC-CM	2.46	rAAV9	hiPSC-CM	1.36
rAAV.KK01	iPSC-CM	17.06	rAAV.KK01	hiPSC-CM	13.68
rAAV.KK02	iPSC-CM	11.86	rAAV.KK02	hiPSC-CM	15.77
rAAV.KK03	iPSC-CM	16.17	rAAV.KK03	hiPSC-CM	14.42
rAAV.KK04	iPSC-CM	22.15	rAAV.KK04	hiPSC-CM	29.37
rAAV.KK05	iPSC-CM	11.39	rAAV.KK05	hiPSC-CM	7.10
rAAV1	hCO	12.00	rAAV1	hCO	1.37
rAAV6	hCO	13.57	rAAV6	hCO	27.62
rAAV9	hCO	2.65	rAAV9	hCO	0.26
rAAV.KK01	hCO	14.36	rAAV.KK01	hCO	8.97
rAAV.KK02	hCO	13.92	rAAV.KK02	hCO	17.21
rAAV.KK03	hCO	13.51	rAAV.KK03	hCO	14.39
rAAV.KK04	hCO	8.37	rAAV.KK04	hCO	20.40
rAAV.KK05	hCO	21.60	rAAV.KK05	hCO	9.80
rAAV1	Human CM 1	16.69	rAAV1	Human CM 1	12.94
rAAV6	Human CM 1	5.40	rAAV6	Human CM 1	7.10
rAAV8	Human CM 1	2.91	rAAV8	Human CM 1	6.01
rAAV9	Human CM 1	3.04	rAAV9	Human CM 1	4.29
rAAV.rh10	Human CM 1	4.21	rAAV.rh10	Human CM 1	14.98
rAAV.rh74	Human CM 1	4.87	rAAV.rh74	Human CM 1	11.71
rAAV.KK01	Human CM 1	33.10	rAAV.KK01	Human CM 1	12.47
rAAV.KK02	Human CM 1	4.79	rAAV.KK02	Human CM 1	4.40
rAAV.KK03	Human CM 1	7.12	rAAV.KK03	Human CM 1	15.61
rAAV.KK04	Human CM 1	12.84	rAAV.KK04	Human CM 1	6.79
rAAV.KK05	Human CM 1	5.03	rAAV.KK05	Human CM 1	3.70
rAAV1	Human CM 2	7.45	rAAV1	Human CM 2	2.10
rAAV6	Human CM 2	6.26	rAAV6	Human CM 2	7.35
rAAV8	Human CM 2	1.10	rAAV8	Human CM 2	16.22
rAAV9	Human CM 2	1.61	rAAV9	Human CM 2	0.45
rAAV.rh10	Human CM 2	1.93	rAAV.rh10	Human CM 2	0.10
rAAV.rh74	Human CM 2	3.22	rAAV.rh74	Human CM 2	0.51
rAAV.KK01	Human CM 2	10.33	rAAV.KK01	Human CM 2	0.77
rAAV.KK02	Human CM 2	6.16	rAAV.KK02	Human CM 2	6.75
rAAV.KK03	Human CM 2	7.92	rAAV.KK03	Human CM 2	2.42
rAAV.KK04	Human CM 2	48.31	rAAV.KK04	Human CM 2	59.55
rAAV.KK05	Human CM 2	5.73	rAAV.KK05	Human CM 2	3.78
rAAV1	Pig CM	4.47	rAAV1	Pig CM	2.48

rAAV6	Pig CM	5.54	rAAV6	Pig CM	24.88
rAAV8	Pig CM	1.02	rAAV8	Pig CM	1.00
rAAV9	Pig CM	1.05	rAAV9	Pig CM	0.56
rAAV.rh10	Pig CM	0.85	rAAV.rh10	Pig CM	0.41
rAAV.rh74	Pig CM	1.28	rAAV.rh74	Pig CM	0.94
rAAV.KK01	Pig CM	64.93	rAAV.KK01	Pig CM	2.44
rAAV.KK02	Pig CM	6.60	rAAV.KK02	Pig CM	24.08
rAAV.KK03	Pig CM	5.55	rAAV.KK03	Pig CM	18.50
rAAV.KK04	Pig CM	3.32	rAAV.KK04	Pig CM	17.91
rAAV.KK05	Pig CM	5.39	rAAV.KK05	Pig CM	6.80
rAAV1	Mouse heart	4.29	rAAV1	Mouse heart	1.25
rAAV6	Mouse heart	3.56	rAAV6	Mouse heart	4.83
rAAV8	Mouse heart	12.08	rAAV8	Mouse heart	15.11
rAAV9	Mouse heart	10.92	rAAV9	Mouse heart	35.24
rAAV.rh10	Mouse heart	13.44	rAAV.rh10	Mouse heart	15.23
rAAV.rh74	Mouse heart	16.14	rAAV.rh74	Mouse heart	14.33
rAAV.KK01	Mouse heart	1.67	rAAV.KK01	Mouse heart	1.25
rAAV.KK02	Mouse heart	3.38	rAAV.KK02	Mouse heart	4.26
rAAV.KK03	Mouse heart	25.26	rAAV.KK03	Mouse heart	3.37
rAAV.KK04	Mouse heart	6.98	rAAV.KK04	Mouse heart	3.31
rAAV.KK05	Mouse heart	2.28	rAAV.KK05	Mouse heart	1.83
rAAV1	NHP CM	11.71	rAAV1	NHP CM	1.44
rAAV6	NHP CM	18.49	rAAV6	NHP CM	7.00
rAAV9	NHP CM	0.78	rAAV9	NHP CM	2.14
rAAV.KK01	NHP CM	24.47	rAAV.KK01	NHP CM	1.14
rAAV.KK02	NHP CM	22.37	rAAV.KK02	NHP CM	8.33
rAAV.KK03	NHP CM	3.76	rAAV.KK03	NHP CM	1.67
rAAV.KK04	NHP CM	9.13	rAAV.KK04	NHP CM	1.77
rAAV.KK05	NHP CM	9.29	rAAV.KK05	NHP CM	2.47